Eur Spine J (2014) 23:2594–2602
DOI 10.1007/s00586-014-3580-8

REVIEW ARTICLE

A comprehensive review of thoracic deformity parameters in scoliosis

Jonathan A. Harris · Oscar H. Mayer · Suken A. Shah · Robert M. Campbell Jr. · Sriram Balasubramanian

Received: 25 November 2013 / Revised: 6 September 2014 / Accepted: 7 September 2014 / Published online: 20 September 2014
© Springer-Verlag Berlin Heidelberg 2014

Abstract
Purpose The combined spine and rib cage deformity in scoliosis is best described as a *thoracic deformity*, and recent advances in imaging have enabled better definition of three-dimensional (3D) deformity of the thorax in scoliosis. However, a comprehensive report that summarizes the published thorax deformity quantification parameter studies is lacking in the orthopaedic literature.
Methods An extensive literature review on the quantification of thorax deformity was performed, and a total of 25 thorax deformity parameters were compiled into eight independent categories based on their similarities of deformity assessment.
Results This review serves as the first comprehensive summary of radiographic and CT-based thorax deformity quantification measures.
Conclusions Future work on the complex relationships between spine and ribcage deformity and the relationship with pulmonary function could help improve clinical interventions for scoliosis treatment.

J. A. Harris · S. Balasubramanian (✉)
School of Biomedical Engineering, Science and Health Systems, Drexel University, 3141 Chestnut Street, Bossone 718, Philadelphia, PA 19104, USA
e-mail: sb939@drexel.edu

O. H. Mayer
Division of Pulmonary Medicine, The Children's Hospital of Philadelphia, Philadelphia, PA, USA

S. A. Shah
Department of Orthopaedic Surgery, Nemours/Alfred I. duPont Hospital for Children, Wilmington, DE, USA

R. M. Campbell Jr.
Division of Orthopaedics, The Children's Hospital of Philadelphia, Philadelphia, PA, USA

Keywords Scoliosis · Thorax deformity · Thoracic insufficiency syndrome · Computer tomography parameters · Radiographic parameters

Introduction

Scoliosis, which affects six to nine million individuals in the United States [1–4], is defined by the Cobb angle of spine curvature in the coronal plane, and is often accompanied by vertebral rotation in the transverse plane and hypokyphosis in the sagittal plane. Although the coronal plane deformity is the main concern in the diagnosis of scoliosis, this complex three-dimensional thoracic deformity affects both the spinal column and the rib cage due to secondary anatomical interconnections [2–8]. These abnormalities in the spine, costal-vertebral joints, and the rib cage produce a 'convex' and 'concave' hemithorax [9, 10], and sternal deviation relative to the apical vertebrae helps define the transverse plane rotational deformity [11]. If thoracic deformity progresses to the point that respiration, lung growth or biomechanical motions are compromised, the condition is called thoracic insufficiency syndrome (TIS) [12].

Historically, the treatment for progressive adolescent idiopathic scoliosis AIS has been spinal fusion with instrumentation, which primarily aims to restore a balanced spine position [13]. With more severe cases of scoliosis, thoracoplasty and rib resection are performed to help reconstruct the thoracic cage to correct the thoracic distortion [14–16]. To support this correction and to preserve spine growth, the vertical expandable prosthetic titanium rib (VEPTR) has been used to preserve spinal and thoracic growth in children too young to be candidates for fusion [17, 18]. While physical therapy and bracing are used to

treat milder forms of scoliosis to maintain cosmesis and avoid surgery [19], the intended goals of acute surgical interventions are to address not only the skeletal deformities, but also the functional outcomes. Determining the optimal time to intervene, however, requires a broad understanding of both the underlying thoracospinal disorder, its progression, and how it impacts pulmonary function. There is a paucity of information on the inter-relationship between spine deformities, thoracic cage shape and pulmonary function.

Despite extensive literature emphasizing the 3D complexity of AIS and subsequent rib cage deformity [11, 20–32], current pre-surgical planning uses 2D coronal and sagittal plane radiographs to assess deformity. In an effort to characterize vertebral, spinal, and rib cage deformity in the transverse plane, several thorax deformity parameters have been proposed in the literature [11, 20–32]. A large discontinuity exists between the scoliosis research society (SRS) glossary of spine deformity and the published thorax deformity quantification parameter studies. While the SRS glossary is an extensive compendium on spine deformity evaluation methods, it does not include thorax deformity measures and their respective correlations with spine deformity [33]. A comprehensive collection of both spine and thorax deformity parameters along with their associated correlations is required to better describe these 3D deformities. This review serves as a collection of radiographic and CT-based parameters developed to assess thoracic deformity organized by similar features.

Methods

A comprehensive search was performed using the PUBMED search engine for publications on radiographic and CT-based parameters developed in the assessment of the skeletal deformities associated with scoliosis. The PUBMED search engine was mined using the following key words in various combinations: scoliosis, thorax deformity, thoracic insufficiency syndrome, computer tomography parameters, and radiographic parameters. Articles not written in English were excluded.

Results

Thorax deformity in the anterior-posterior and medial—lateral planes is primarily assessed for clinical purposes using planar radiographs [11, 26, 28, 31]. CT imaging, the gold standard for transverse plane thorax deformity characterization, is also used to complement AP and lateral radiographs [6, 20, 22–29, 31]. A comprehensive literature review on the quantification of thorax deformity was performed, and a total of 25 thorax deformity parameters were compiled into eight independent categories based on their similarities of deformity assessment (Table 1). The categories of thorax deformity (in alphabetical order) are: (1) Anterior chest angulation, (2) Area enclosed by rib cage, (3) Coronal asymmetry, (4) Hemithorax depth asymmetry, (5) Hemithorax width asymmetry, (6) Posterior rib asymmetry, (7) Sagittal depth, and (8) Sternum deviation. Figure 1 describes the anatomical landmarks used to quantify thorax deformity using radiographic and CT-based measures.

Relationship of thorax deformity parameters with Cobb angle and vertebral rotation

Scoliosis-induced lateral spine curvature in the coronal plane and vertebral rotation are commonly used for clinical assessment and their inter-relationship has been widely documented [6, 26, 27, 30, 31, 34]. Furthermore, additional evidence supports the subsequent contribution of spine distortion towards progression of thoracic cage deformity [2–5]. It is important to understand the associations that may exist between primary spine deformity and secondary thorax deformity parameters to validate and establish clinical relevance. Therefore, a comprehensive literature review was performed to study the established relationships of thorax deformity parameters with spine curvature and vertebral rotation. The results are organized by thorax deformity category and are summarized below.

Anterior chest angulation

Anterior chest wall angle was shown to significantly correlate with Cobb angle ($r = 0.377$, $p < 0.001$), but not with vertebral rotation [27]. It also noted that the most severe anterior chest wall deformity occurred in patients with the apical level at T9. Sternal Tilt was developed by Hong et al. [24] to measure the angulation of the sternum in PE patients with AIS. However, Sternal Tilt did not correlate to Cobb angle and its relationship with vertebral rotation has not been studied. Angle of Sternum Relative to Apical Vertebrae was found to significantly correlate with Cobb angle and vertebral rotation ($r = -0.401$, $p < 0.001$ and $r = -0.757$, $p < 0.001$, respectively) [27]. Despite coupling that may exist between apical vertebral rotation, rib head deformity, and anterior chest angulation in AIS, the aforementioned literature data may be influenced by the causal nature of vertebral rotation on the angle of sternum relative to apical vertebrae.

Area enclosed by rib cage

Kyphosis-lordosis index from T6–T12 have been shown to significantly correlate with Cobb angle ($r = -0.25$ to

Table 1 Radiographic and CT-based thorax deformity parameters

Deformity feature	Parameter	Definition	Landmark equivalent
Anterior chest angulation	Angle of sternum rel. to apical vertebrae [27]	Angle formed between horizontal line bisecting sternum and vertebral bisectional line	Line 1: Sternum bisectional plane line 2: Apical VB bisectional plane
	Anterior chest wall angle [27]	Angle between frontal plane and oblique plane through the concave and convex anterior costal projects and the frontal plane	
	Sternal tilt [24]	Angle formed between frontal plane and horizontal line bisecting sternum	Line 1: sternum bisectional plane Line 2: *X*-axis
Area enclosed by rib cage	Frontosagittal index [25]	Ratio of Sternovertebral distance over transverse diameter as a percentage	$AJ_y/TE_x \times 100\ \%$
	Haller index [25]	Ratio of transverse diameter over sternovertebral distance	TE_x/AJ_y
	Kyphosis-Lordosis index [20]	Ratio of sagittal diameter over transverse diameter	AJ_y/TE_x
	Pectus index [23]	Ratio of transverse diameter over sternovertebral distance	TE_x/AJ_y
	Transverse diameter [20]	Maximum distance along frontal plane projected through most lateral interior aspects of the costal at apical level	TE_x
Coronal asymmetry	[a]Apical rib vertebral angle difference [28]	A perpendicular line is drawn to the middle of either the upper or lower border o the apical vertebrae. Another line is drawn from the mid-point of the head of the rib to the mid-point of the neck of the rib, just medial to the region where the neck widens into the shaft of the rib. The rib line is extended medially to intersect the vertebral line to make the rib vertebrae angle	$K'L'_x$ and $I'J'_x$
	[a]Space Available for Lung [11]	Referencing an AP radiograph, the height of the hemithorax is defined as the distance from the middle of the most cephalad rib down to the center of the hemidiaphragm. A ratio, expressed as a percentage, is derived by dividing the height of the concave hemithorax by the height of the convex hemithorax, defining the space available for the lung	$A'B'_x$ and $C'D'_x$
Hemithorax depth asymmetry	Asymmetry index [25]	Ratio of maximum left and right AP hemithorax diameters at apical level subtracted from 1	$1-(QU_x/HC_x)$
	Chest asymmetry [24]	Absolute difference between maximum AP distances of right and left hemithorax	$\lvert QU_x - HC_x \rvert$
	Chest flatness index [25]	Ratio of twice the maximum transverse diameter and the sum of both maximum AP hemithorax diameters at apical level	$2 \times TE_x/(QU_x - HC_x)$
Hemithorax width asymmetry	[a]Apical vertebral body-rib ratio [26]	The ratio of linear measurements (larger over smaller distance) from the lateral borders of the apical thoracic vertebrae to the chest wall on an AP radiograph	$E'F'_x$ and $G'H'_x$
	Posterior hemithoracic symmetry ratio [11]	Distance between interior surface and anterior tip of the costal at the costovertebral articulation along oblique plane through tips. Ratio calculated by dividing smallest distance from largest	PO_x and DI_x
	Sternum-rib ratio [27]	Convex/Concave ratio of linear measurements from midpoint of the sternum to exterior of rib cage along frontal plane at apical level	BS_x and BF_x

Table 1 continued

Deformity feature	Parameter	Definition	Landmark equivalent
Posterior rib asymmetry	Angle of trunk rotation [22]	Angle formed between frontal plane and tangential line drawn to the posterior rib hump deformity	
	Posterior rib rotation [30]	Angle between frontal plane and oblique plane traveling through posterior apexes of costals at apical level	
	[b]Rib hump [26]	Linear distance between the left and right posterior rib prominences at the apex of the rib deformity on a lateral radiograph	Not shown in figure
	Rib hump index [20]	Ratio H–D/W, where H is distance from frontal plane through the posterior central point of the vertebral foramen to the apex of the inner costal hump. D is the same measurement on the concave hemithorax. W is the distance between the sagittal planes traveling through both the apex of the convex costal and posterior central point of the vertebral foramen at the apical level	$H = \mathrm{LQ_y}$ (convex) $D = \mathrm{LH_y}$ (*concave*) $W = \mathrm{LQ_x}$ (convex)
	Rib hump index [31]	Ratio $(\mathrm{H_1} - \mathrm{H_2})/_{W} \times 100\,\%$, where $\mathrm{H_1}$ is distance from frontal plane through the posterior central point of the vertebral foramen to the apex of the inner costal hump. $\mathrm{H_2}$ is the same measurement on the concave hemithorax. W is the distance between interior extremes along frontal plane bisecting posterior most point of foramen at the apical level	$H_1 = \mathrm{LQ_y}$ (convex) $H_2 = \mathrm{LH_y}$ (*concave*) $W = \mathrm{RG_x}$
Sagittal depth	Sagittal diameter [20]	Distance between posterior midpoint of sternum and anterior point of foramen along AP Plane	$\mathrm{AL_y}$
	Sternovertebral distance [25]	Distance between posterior midpoint of sternum and anterior point of apical vertebrae along AP Plane	$\mathrm{AJ_y}$
Sternum deviation	Midline deviation [20]	Angle between AP plane and line through posterior aspect of foramen and anterior midpoint of sternum	Line 1: *Y*-axis line 2: NA
	Thoracic rotation [11]	Angle between plane bisecting sternum and anterior aspect of vertebral body and plane bisecting vertebrae	Line 1: Apical vert. bisectional line Line 2: BM
	Vertebral translation [6]	Distance between AP planes though center of foramen and bisecting sternum	$\mathrm{BM_x}$

[a] Measurements from AP radiograph

[b] Measurements from lateral radiograph

Apical Transverse Plane Landmarks	
A	Center of Posterior Sternal Surface
B	Centroid of Sternum
U:Q	Maximum Left AP Hemi-diameter
C:H	Maximum Right AP hemi-diameter
T:E	Maximum Interior Transverse Diameter
S	Lateral-Most Point of Left Costal
F	Lateral-Most Point of Right Costal
J	Anterior-Point Point of Apical VB
L	Anterior-Most Point of Foramen
M	Centroid of Foramen
N	Posterior-Most Point of Foramen
K	Anterior-Most Point of Apical VB Along Bi-sectional Line
O	Anterior-Most Point of Left Costal
I	Anterior-Most Point of Right Costal
P	Lateral-Most Left Interior Point Along Plane Bisecting O-I
D	Lateral-Most Right Interior Point Along Plane Bisecting O-I
R	Lateral-Most Left Interior Point Along Plane Bisecting N
G	Lateral-Most Right Interior Point Along Plane Bisecting N
V	Posterior-Most Point of Left Apical Rib
W	Posterior-Most Point of Right Apical Rib

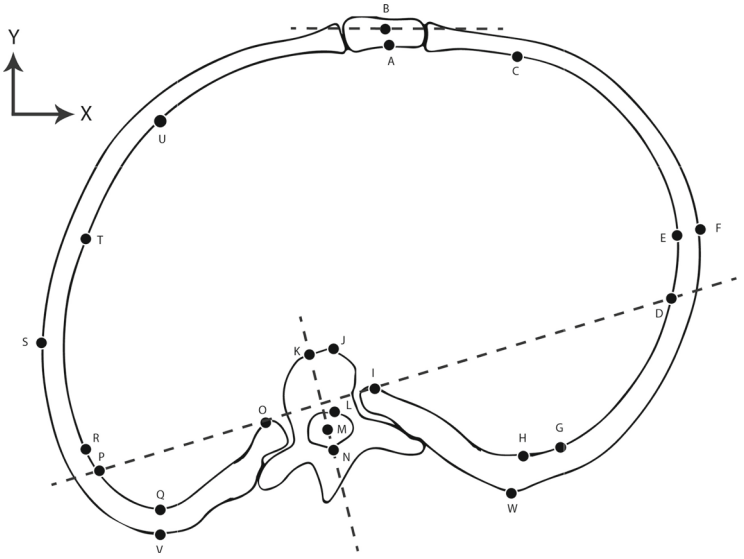

Coronal Radiographic Landmarks	
A’	Centroid of Left Cephalic Rib
B’	Center of Left Hemi-Diaphragm
C’	Centroid of Right cephalic Rib
D’	Center of right Hemi-Diaphragm
G’	Lateral-Most Left Point of Apical VB
H’	Lateral-Most Left Point at G’
E’	Lateral-Most Right Point of Apical VB
F’	Lateral-Most Right Point at E’
K’:L’	Points along Apical Left Costal Bisect Line
I’:J’	Points along Apical Right Costal Bisect Line

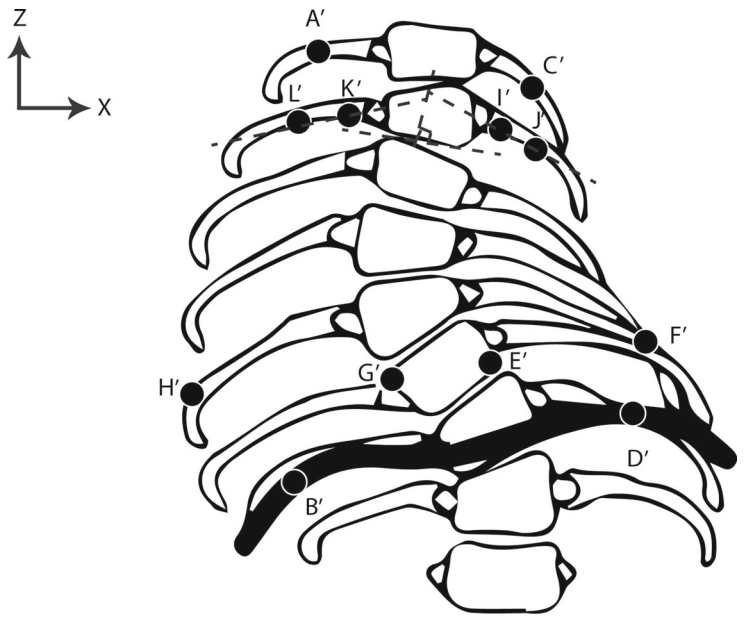

Fig. 1 Radiographic and CT-Based landmark data

−0.405, $p < 0.01$), but was not studied to correlate with vertebral rotation [31]. However, no significant correlation was observed between pectus index [23] and Cobb angle or vertebral rotation [24]. Haller index [25], Frontosagittal index [25], and transverse diameter [20] were not studied to correlate with either Cobb angle or vertebral rotation.

Coronal asymmetry

Apical rib vertebral angle difference did not significantly correlate with Cobb angle or vertebral rotation [26]. The relationship between space available for the lung and spine deformity measures have not yet been studied.

Hemithorax depth asymmetry

CT-based measures are used to clinically assess hemithorax depth asymmetry in pectus excavatum (PE) patients. PE is a congenital anterior thoracic cage deformity that has been shown to affect cardiopulmonary function due to the significant reduction in chest volume. While there exists a 22.58 % increase (38.46 % for female) in incidence of adolescent idiopathic scoliosis (AIS) within the PE population [24], hemithorax depth asymmetry measurements are not assessed in AIS subjects. So, there is a lack of correlative analysis associating asymmetry index, chest asymmetry index, and chest flatness index with lateral curvature or vertebral rotation.

Hemithorax width asymmetry

Sternum-rib ratio was shown to significantly correlate with both Cobb angle and vertebral rotation ($r = 0.514$, $p < 0.001$ and $r = 0.213$, $p < 0.05$, respectively) [27]. Apical vertebral body-rib ratio was also found to correlate with Cobb and vertebral rotation ($r = 0.57$, $p < 0.005$ and $r = 0.49$, $p < 0.005$, respectively) [26]. Posterior hemithoracic symmetry ratio [11] has not been assessed for its relationship with Cobb angle or vertebral rotation.

Posterior rib rotation

The rib hump index originally defined by Aaro et al. [20] but later modified by Takahashi et al., both consider laterolateral axis width measurements and showed significant correlation with lateral spine curvature (Aaro: $r = 0.601$, $p < 0.001$, Takahashi: T6–T12, $r = 0.306$–0.507, $p < 0.001$) and vertebral rotation (Aaro: $r = 0.36$, $p < 0.02$, Takahashi: not studied) [20, 30, 31]. Rib hump, based on lateral radiographic measurements was shown to correlate with Cobb angle ($r = 0.65$, $p < 0.0001$) and vertebral rotation ($r = 0.53$, $p < 0.002$) [26]. If vertebral rotation leads to rib deformity, the most deformed ribs would be coupled with the apical vertebrae. However, there exists a systematic flaw in the use of CT-based measurements to assess posterior rib asymmetry, in that the posterior ribs observed in the axial 'slices' through the apical vertebrae connect to vertebrae superior to the apical vertebrae due to the natural droop of the costals.

Posterior rib rotation and back surface rotation demonstrated significant correlation with Cobb angle ($r = 0.63$ and 0.88 respectively, $p < 0.05$) and vertebral rotation ($r = 0.63$ and 0.77 respectively, $p < 0.05$) [30]. While Mao et al. reported a significant correlation between Cobb angle and Angle of Trunk rotation ($r = 0.517$, $p < 0.05$); Erukla et al. did not observe any relationship. More recently, Carlson et al. [21] used a Bunnell scoliometer to measure Angle of Trunk Inclination and found significant correlations with Cobb angle ($r = 0.711$, $p < 0.004$) and vertebral rotation ($r = 0.53$, $p < 0.02$).

Sagittal depth

Takahashi et al. [31] assessed the sagittal diameter at every vertebral level, and reported significant negative correlations between sagittal diameter and lateral curvature at the apical vertebra (T9: $r = -0.218$, $p < 0.022$) and the adjacent vertebral levels. Although not quantitatively assessed, it was also noted that vertebral rotation was most severe at the same vertebral levels that corresponded with sagittal diameter [31]. Sternovertebral distance [25] has never been correlated with Cobb or vertebral rotation.

Sternum deviation

Midline deviation was shown to significantly correlate with Cobb angle ($r = 0.76$, $p < 0.01$) [20, 34] and was not studied further to determine relationship with vertebral rotation. Vertebral translation has been shown to correlate significantly with both Cobb angle and vertebral rotation ($r = 0.657$, $p < 0.001$ and $r = 0.317$, $p < 0.006$, respectively) [6]. The relationships between thoracic rotation [11] and either Cobb angle or vertebral rotation have not been studied.

Discussion

Three-dimensional imaging methods and deformity characterization are essential in guiding surgical restoration of abnormal spine curvature, thoracic volume, symmetry, and function [35]. CT and MRI techniques may provide a level of detail needed to assess out-of-plane spine rotation and thoracic volume changes that often accompany scoliosis. Currently, AP radiography is the gold standard to assess scoliosis, and it is a favored imaging method due to low radiation exposure, making it very practical for longitudinal observations. Although sufficient in assessing spine curvature in the coronal and sagittal planes, AP radiographs are inadequate for describing the vertebral rotation and rib cage distortions; which can be better assessed using transverse plane measurements [20].

The current literature on scoliosis-induced thorax deformity characterization is mainly focused on CT-derived transverse plane measurements. Due to the more pronounced caudal rotation of the ribs in scoliosis, a transverse image alone may not capture the true thoracic distortion of the deformity [34]. With a limited number of studies evaluating the relationship of transverse measurements with AP and lateral radiographs, a comprehensive understanding of the 3D thoracic deformity does not exist [6]. Such knowledge is especially critical, and timely, since we routinely use space available for the lung (SAL), a 2D assessment as a preoperative indicator for VEPTR implantation [11]. Although the VEPTR corrects hemithorax height asymmetry in the coronal plane, the impact of such correction on thoracic measurements in the transverse plane has not been well-studied.

With these limitations, AP radiographs are still used to assess and describe scoliosis-induced thorax deformity with parameters such as rib hump, apical vertebral body-rib ratio, rib-vertebral angle difference and space available for the lung [11, 26, 28]; measures used as proxy for 3D thorax deformity characterization without sufficient validation in the literature. While rib hump and apical vertebral body-rib ratio were shown to correlate significantly with Cobb angle and vertebral rotation. There was no correlation between Cobb angle and there were no comparisons made between Cobb angle and Space Available for the Lung [26, 28]. These findings indicate the inherent limitations of 2D imaging-based measures in describing a 3D deformity.

The current review of thorax deformity quantification presents only 2D measures derived from 3D imaging, and subsequently does capture the true 3D thorax deformity. To our knowledge, crude thoracic volume index (CTVI) is the only parameter that assesses 3D volume related changes in the thorax [36], and was shown to correlate well with functional pulmonary output. Future studies could combine planar data derived from any imaging modality to comprehensively describe changes in thoracic volume.

While surgical interventions for scoliosis primarily focus on correcting abnormal spine curvature, the ultimate goal is to restore thoracic function, assessed by improvements in thorax geometry, rib cage motion and pulmonary function [37, 38]. The impact of 2D geometry measurements on rib cage motion and thoracic biomechanics is incomplete. Although the effect of 2D deformity measures such as Cobb angle and vertebral rotation on pulmonary function has been extensively studied, these efforts do not take into consideration the interplay between spine deformity and subsequent thorax distortion [38–41]. Upadhyay et al. [40] reported that the patients with rotational flexibility less than 55 %, thoracic kyphosis less than 15°, and rib-vertebral angle asymmetry greater than 25° had relatively poor pulmonary function; with 85 % of patients meeting two of the three measurements having a vital capacity of 70 % or less of their predicted values. While these data could significantly contribute towards clinical prognosis, they provide limited information to further our understanding of changes in pulmonary function due to 3D thorax deformity.

Although radiographic measurements are clinically the most feasible, the development of 3D geometric characterization based on imaging modalities such as CT and dynamic MRI may be valuable. However, with CT-based methods, there is a growing concern related to an increased risk of radiation in children whose conditions may require longitudinal imaging studies. More recently, optimization of CT radiation dosage and scan speed have successfully shown to reduce radiation exposure of the whole spine from an average effective dose of 6 to 0.3 mSv without compromising effective clinical evaluation of scoliotic deformity [42].

Despite these advances in CT protocol, radiation exposure still remains 2–3 times greater than that of a plain radiograph for the whole spine. Additionally, there may be measurement errors due to subject position–i.e. standing versus supine [20]. In comparison with standing radiographic measurements of Cobb angle and vertebral rotation, Yazici et al. [43] observed a 29.78 % and 24.39 % decrease when the patients were imaged using a supine CT. More recently, Lee et al. [44] also reported that a supine MRI underestimate Cobb angle measured using radiographs by an average of 10°. However, these results may be confounded by differences in imaging modalities used. Alleviating radiation and subject-position related limitations, newer imaging methods such as EOS® (EOS Imaging, Paris, France) offer high-quality biplanar radiographs of the entire body in the standing position with an ultra-low radiation dose [45, 46]. Whole-body, weight bearing, erect radiographs provide accurate relationships of scoliotic deformities, compensatory curves, global sagittal balance, trunk and rib cage relationships, and describe the complex interplay of the spine and pelvic (pelvic incidence) [47–50]. While current dynamic MRI techniques enable position- and time-variant functional assessment of the spine and thorax with no radiation exposure, future advancements in medical image processing methods may also help render real-time biplanar radiograph-based deformity characterization [51–53].

Conclusion

Practitioners and researchers involved in the treatment of children with scoliosis need to have a thorough understanding of the three-dimensional nature of scoliosis and other spinal deformities and relative changes in the rib cage

and thorax. This review serves as the first comprehensive summary of thorax deformity quantification measures. Continued development of advanced imaging and further work in uncovering the complex relationships of spinal deformity, rib cage development and pulmonary function will optimize the treatment of these children and improve their quality of life.

Acknowledgments We would like to acknowledge James Peters and Reese Juelg for creating the illustrations used in this paper.

Conflict of interest None.

References

1. Roaf R (1966) The basic anatomy of scoliosis. J Bone Joint Surg Br 48(4):786–792
2. Lenke LG, Betz RR, Harms J, Bridwell KH, Clements DH, Lowe TG, Blanke K (2001) Adolescent idiopathic scoliosis: a new classification to determine extent of spinal arthrodesis. J Bone Joint Surg Am 83-A(8):1169–1181
3. Stokes IA (1994) Three-dimensional terminology of spinal deformity. A report presented to the Scoliosis Research Society by the Scoliosis Research Society Working Group on 3-D terminology of spinal deformity. Spine 19(2):236–248
4. Weinstein SL, Dolan LA, Cheng JC, Danielsson A, Morcuende JA (2008) Adolescent idiopathic scoliosis. Lancet 371(9623): 1527–1537. doi:10.1016/S0140-6736(08)60658-3
5. Cobb JRM (1948) Outline For The Study of Scoliosis. Paper presented at the The American Academy of Orthopaedic Surgeons
6. Easwar TR, Hong JY, Yang JH, Suh SW, Modi HN (2011) Does lateral vertebral translation correspond to Cobb angle and relate in the same way to axial vertebral rotation and rib hump index? A radiographic analysis on idiopathic scoliosis. Eur Spine J 20(7):1095–1105. doi:10.1007/s00586-011-1702-0
7. Gervais J, Perie D, Parent S, Labelle H, Aubin CE (2012) MRI signal distribution within the intervertebral disc as a biomarker of adolescent idiopathic scoliosis and spondylolisthesis. BMC Musculoskeletal Disord 13:239. doi:10.1186/1471-2474-13-239
8. Di Silvestre M, Lolli F, Bakaloudis G, Maredi E, Vommaro F, Pastorelli F (2013) Apical vertebral derotation in the posterior treatment of adolescent idiopathic scoliosis: myth or reality? Eur Spine J 22(2):313–323. doi:10.1007/s00586-012-2372-2
9. Thulbourne T, Gillespie R (1976) The rib hump in idiopathic scoliosis. Measurement, analysis and response to treatment. J Bone Joint Surg Br 58(1):64–71
10. Grivas TB, Vasiliadis ES, Mihas C, Savvidou O (2007) The effect of growth on the correlation between the spinal and rib cage deformity: implications on idiopathic scoliosis pathogenesis. Scoliosis 2:11. doi:10.1186/1748-7161-2-11
11. Campbell RM Jr, Smith MD, Mayes TC, Mangos JA, Willey-Courand DB, Kose N, Pinero RF, Alder ME, Duong HL, Surber JL (2003) The characteristics of thoracic insufficiency syndrome associated with fused ribs and congenital scoliosis. J Bone Joint Surg Am 85-A(3):399–408
12. Campbell RM Jr, Adcox BM, Smith MD, Simmons JW 3rd, Cofer BR, Inscore SC, Grohman C (2007) The effect of mid-thoracic VEPTR opening wedge thoracostomy on cervical tilt associated with congenital thoracic scoliosis in patients with thoracic insufficiency syndrome. Spine 32(20):2171–2177. doi:10.1097/BRS.0b013e31814b2d6c
13. Youssef DOO JA, Patty CA, Scott MA, Price HL, Hamlin LF, Williams TL, Uribe JS, Deviren V (2013) Current status of adult spinal deformity. Global Spine J 1(3):51–62. doi:10.1055/s-0032-1326950
14. Bullmann V, Schulte TL, Schmidt C, Gosheger G, Osada N, Liljenqvist UR (2013) Pulmonary function after anterior double thoracotomy approach versus posterior surgery with costectomies in idiopathic thoracic scoliosis. Eur Spine J 22(Suppl 2):S164–S171. doi:10.1007/s00586-012-2316-x
15. Yang JH, Bhandarkar AW, Kasat NS, Suh SW, Hong JY, Modi HN, Hwang JH (2013) Isolated percutaneous thoracoplasty procedure for skeletally mature adolescent idiopathic scoliosis patients, with rib deformity as their only concern: short-term outcomes. Spine 38(1):37–43. doi:10.1097/BRS.0b013e3182784cdc
16. Shi Z, Wu Y, Huang J, Zhang Y, Chen J, Guo K, Li M, Ran B (2013) Pulmonary function after thoracoplasty and posterior correction for thoracic scoliosis patients. Int J Surg. doi:10.1016/j.ijsu.2013.05.035
17. Ramirez N, Flynn JM, Serrano JA, Carlo S, Cornier AS (2009) The Vertical Expandable Prosthetic Titanium Rib in the treatment of spinal deformity due to progressive early onset scoliosis. J Pediatr Orthop B 18(4):197–203. doi:10.1097/BPB.0b013e32832bf5e0
18. Skaggs DL, Akbarnia BA, Flynn JM, Myung KS, Sponseller PD, Vitale MG, Approved by the Chest W, Spine Deformity Study Group tGSSGPOSoNA, the Scoliosis Research Society Growing Spine Study C (2013) A classification of growth friendly spine implants. J Pediatr Orthop. doi:10.1097/BPO.0000000000000073
19. Stokes OM, Luk KD (2013) The current status of bracing for patients with adolescent idiopathic scoliosis. Bone Joint J 95-B(10):1308–1316. doi:10.1302/0301-620X.95B10.31474
20. Aaro S, Dahlborn M (1981) Estimation of vertebral rotation and the spinal and rib cage deformity in scoliosis by computer tomography. Spine 6(5):460–467
21. Carlson BB, Burton DC, Asher MA (2013) Comparison of trunk and spine deformity in adolescent idiopathic scoliosis. Scoliosis 8(1):2. doi:10.1186/1748-7161-8-2
22. Erkula G, Sponseller PD, Kiter AE (2003) Rib deformity in scoliosis. Eur Spine J 12(3):281–287. doi:10.1007/s00586-002-0523-6
23. Haller JA Jr, Kramer SS, Lietman SA (1987) Use of CT scans in selection of patients for pectus excavatum surgery: a preliminary report. J Pediatr Surg 22(10):904–906
24. Hong JY, Suh SW, Park HJ, Kim YH, Park JH, Park SY (2011) Correlations of adolescent idiopathic scoliosis and pectus excavatum. J Pediatr Orthop 31(8):870–874. doi:10.1097/BPO.0b013e31822da7d5
25. Kilda A, Basevicius A, Barauskas V, Lukosevicius S, Ragaisis D (2007) Radiological assessment of children with pectus excavatum. Indian J Pediatr 74(2):143–147
26. Kuklo TR, Potter BK, Lenke LG (2005) Vertebral rotation and thoracic torsion in adolescent idiopathic scoliosis: what is the best radiographic correlate? J Spinal Disord Tech 18(2):139–147
27. Mao SH, Qiu Y, Zhu ZZ, Zhu F, Liu Z, Wang B (2011) Clinical evaluation of the anterior chest wall deformity in thoracic adolescent idiopathic scoliosis. Spine. doi:10.1097/BRS.0b013e31823a05e6
28. Mehta MH (1972) The rib-vertebra angle in the early diagnosis between resolving and progressive infantile scoliosis. J Bone Joint Surg Br 54(2):230–243
29. Ohno K, Nakahira M, Takeuchi S, Shiokawa C, Moriuchi T, Harumoto K, Nakaoka T, Ueda M, Yoshida T, Tsujimoto K, Kinoshita H (2001) Indications for surgical treatment of funnel chest by chest radiograph. Pediatr Surg Int 17(8):591–595. doi:10.1007/s003830100000

30. Stokes IA (1989) Axial rotation component of thoracic scoliosis. J Orthop Res 7(5):702–708. doi:10.1002/jor.1100070511
31. Takahashi S, Suzuki N, Asazuma T, Kono K, Ono T, Toyama Y (2007) Factors of thoracic cage deformity that affect pulmonary function in adolescent idiopathic thoracic scoliosis. Spine 32(1):106–112
32. Williams AM, Crabbe DC (2003) Pectus deformities of the anterior chest wall. Paediatr Respir Rev 4(3):237–242
33. Grivas TB, de Mauroy JC, Negrini S, Kotwicki T, Zaina F, Wynne JH, Stokes IA, Knott P, Pizzetti P, Rigo M, Villagrasa M, Weiss HR, Maruyama T, members S (2010) Terminology-glossary including acronyms and quotations in use for the conservative spinal deformities treatment: 8th SOSORT consensus paper. Scoliosis 5:23. doi:10.1186/1748-7161-5-23
34. Aaro S, Dahlborn M (1981) The longitudinal axis rotation of the apical vertebra, the vertebral, spinal, and rib cage deformity in idiopathic scoliosis studied by computer tomography. Spine 6(6):567–572
35. Campbell RM Jr (2013) VEPTR: past experience and the future of VEPTR principles. Eur Spine J 22(Suppl 2):S106–S117. doi:10.1007/s00586-013-2671-2
36. Mankin HJ, Graham JJ, Schack J (1964) Cardiopulmonary function in mild and moderate idiopathic scoliosis. J Bone Joint Surg Am 46:53–62
37. Campbell RM Jr (2013) VEPTR: past experience and the future of VEPTR principles. Eur Spine J 22(Suppl 2):106–117. doi:10.1007/s00586-013-2671-2
38. Demura S, Bastrom TP, Schlechter J, Yaszay B, Newton PO, Harms Study G (2013) Should postoperative pulmonary function be a criterion that affects upper instrumented vertebra selection in adolescent idiopathic scoliosis surgery? Spine. doi:10.1097/BRS.0b013e3182a637a8
39. Lin MC, Liaw MY, Chen WJ, Cheng PT, Wong AM, Chiou WK (2001) Pulmonary function and spinal characteristics: their relationships in persons with idiopathic and postpoliomyelitic scoliosis. Arch Phys Med Rehabil 82(3):335–341. doi:10.1053/apmr.2001.21528
40. Upadhyay SS, Mullaji AB, Luk KD, Leong JC (1995) Relation of spinal and thoracic cage deformities and their flexibilities with altered pulmonary functions in adolescent idiopathic scoliosis. Spine 20(22):2415–2420
41. Upadhyay SS, Mullaji AB, Luk KD, Leong JC (1995) Evaluation of deformities and pulmonary function in adolescent idiopathic right thoracic scoliosis. Eur Spine J 4(5):274–279
42. Kalra MK, Quick P, Singh S, Sandborg M, Persson A (2013) Whole spine CT for evaluation of scoliosis in children: feasibility of sub-milliSievert scanning protocol. Acta Radiol 54(2):226–230. doi:10.1258/ar.2012.110625
43. Yazici M, Acaroglu ER, Alanay A, Deviren V, Cila A, Surat A (2001) Measurement of vertebral rotation in standing versus supine position in adolescent idiopathic scoliosis. J Pediatr Orthop 21(2):252–256
44. Lee MC, Solomito M, Patel A (2013) Supine magnetic resonance imaging cobb measurements for idiopathic scoliosis are linearly related to measurements from standing plain radiographs. Spine 38(11):E656–E661. doi:10.1097/BRS.0b013e31828d255d
45. McKenna C, Wade R, Faria R, Yang H, Stirk L, Gummerson N, Sculpher M, Woolacott N (2012) EOS 2D/3D X-ray imaging system: a systematic review and economic evaluation. Health Technol Assess 16(14):1–188. doi:10.3310/hta16140
46. Al-Aubaidi Z, Lebel D, Oudjhane K, Zeller R (2013) Three-dimensional imaging of the spine using the EOS system: is it reliable? A comparative study using computed tomography imaging. J Pediatr Orthop B 22(5):409–412. doi:10.1097/BPB.0b013e328361ae5b
47. Glaser DA, Doan J, Newton PO (2012) Comparison of 3-dimensional spinal reconstruction accuracy: biplanar radiographs with EOS versus computed tomography. Spine 37(16):1391–1397. doi:10.1097/BRS.0b013e3182518a15
48. Humbert L, De Guise JA, Aubert B, Godbout B, Skalli W (2009) 3D reconstruction of the spine from biplanar X-rays using parametric models based on transversal and longitudinal inferences. Med Eng Phys 31(6):681–687. doi:10.1016/j.medengphy.2009.01.003
49. Ilharreborde B, Sebag G, Skalli W, Mazda K (2013) Adolescent idiopathic scoliosis treated with posteromedial translation: radiologic evaluation with a 3D low-dose system. Eur Spine J. doi:10.1007/s00586-013-2776-7
50. Ilharreborde B, Vidal C, Skalli W, Mazda K (2013) Sagittal alignment of the cervical spine in adolescent idiopathic scoliosis treated by posteromedial translation. Eur Spine J 22(2):330–337. doi:10.1007/s00586-012-2493-7
51. Yang Y, Van Reeth E, Poh CL, Tan CH, Tham I (2013) A spatio-temporal based scheme for efficient registration-based segmentation of thoracic 4D MRI. IEEE J Biomed Health Inform. doi:10.1109/JBHI.2013.2282183
52. Bagci U, Foster B, Miller-Jaster K, Luna B, Dey B, Bishai WR, Jonsson CB, Jain S, Mollura DJ (2013) A computational pipeline for quantification of pulmonary infections in small animal models using serial PET-CT imaging. EJNMMI Res 3(1):55. doi:10.1186/2191-219X-3-55
53. Li G, Citrin D, Camphausen K, Mueller B, Burman C, Mychalczak B, Miller RW, Song Y (2008) Advances in 4D medical imaging and 4D radiation therapy. Technol Cancer Res Treat 7(1):67–81